Generating a Large-scale Numerical Database of Motor Vehicle Crashes for Rapid Injury Severity Prediction

Wentao Chen, Qing Zhou, Shun Gan, Bingbing Nie

I. INTRODUCTION

Reducing the occurrence and injury severity of motor vehicle crashes (MVCs) is a major topic in the traffic safety area [1]. Accurate and rapid occupant injury risk prediction can largely benefit integrated safety systems. Existing prediction models mostly use factors available in police accident reports, which cannot cover all of the significant influencing factors prior to collision. Real-time and purpose-specific prediction models (e.g. deep learning) have demonstrated the potential for improving accuracy with application to MVCs when training data is sufficient [2]. For the data collection, Naturalistic Driving Data (NDD) have been widely used for training real-time accident occurrence prediction models, but NDD is not suitable for injury severity prediction since it only contains a small portion of MVCs. A reliable database that can supply systematic in-crash injury information to NDD has the potential to bridge this gap by separating the near-crash phase from the in-crash phase. This study developed a framework in generating a large-scale numerical database for training rapid injury prediction algorithims when the data is being used in combination with NDD (Fig. 1). The multi-level input features that can be measured or predicted with NDD include initial impact condition, restraint system configurations and driver characteristics. The outputs are the driver injury severity of different body regions. The credibility of the database was validated against real-world MVCs.

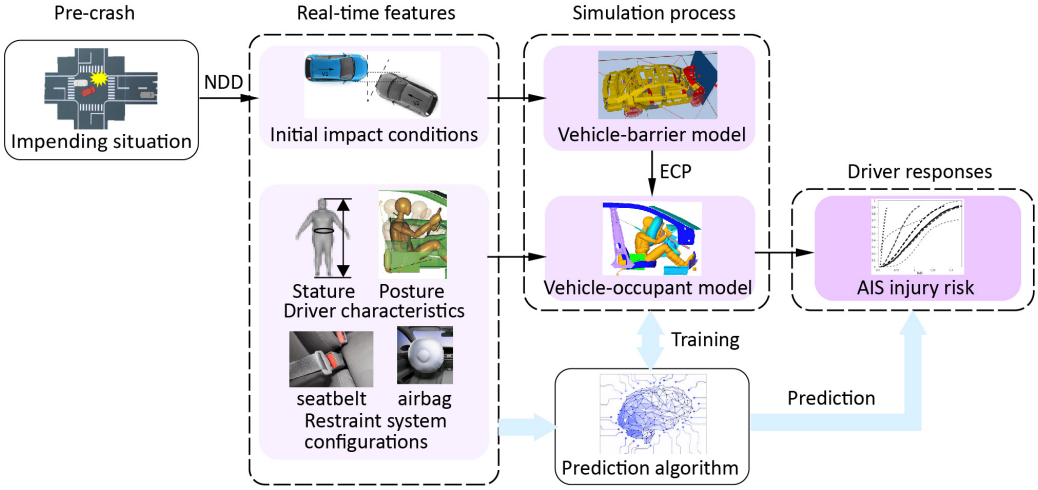

Fig. 1. The framework of generating a rapid injury severity prediction using a combined database on near-crash naturalist driving and in-crash occupant responses (the relevant work to the present study is marked in solid background).

II. METHODS

We used two highly computational-efficient software (i.e. Visual Crash Studio (VCS) and MAthematical DYnamic Models (MADYMO)) to build a large-scale numerical database of MVCs. The collision event was divided into two phases (Fig. 1): the first impact phase, i.e. the impact between the vehicle to exterior object; and the second impact phase, i.e. the impact between in-vehicle occupants and interior. For the first impact phase, the vehicle-rigid wall impact condition was used for simplification purposes. We used the vehicle-barrier model under the VCS environment to generate Equivalent Crash Pulse (ECP) and then imported the ECP, driver characteristics and restraint system configurations into the vehicle-occupant model under MADYMO environment to calculate

B. Nie (e-mail: nbb@tsinghua.edu.cn; tel: +86-10-6278-8689) is an Associate Professor of Mechanical Engineering, W. Chen and S. Gan are PhD students in Mechanical Engineering, Q. Zhou is a Professor of Mechanical Engineering, all in the School of Vehicle and Mobility at Tsinghua University, China.

the driver injury severity. A representative sedan model, i.e. TOYOTA Camry 2012, was selected as the target vehicle. The simulation model was validated against selected real-world MVCs.

Baseline model establishment A finite element (FE) model of Camry developed by George Mason University [3] served as the reference model. The VCS baseline model, which includes the main force transmission path of the vehicle, was constructed with beam and rigid-body structures. The baseline model was validated against three different impact results of the FE model (i.e. 64 km/h full frontal impact, 45 km/h full frontal impact, and 35 km/h small-angle offset impact) and a Camry 35 mph NCAP frontal impact test performed by NHTSA (Test number 6953). The MADYMO baseline model interior space was imported from the FE model. For validation purposes, the dummy response curves were compared with the corresponding physical tests regarding the main output responses, i.e. head linear acceleration, chest acceleration, chest deflection, neck force, neck moment, femur axial force and tibia axial force.

Features definition (inputs)

First impact phase The input features to configure the impact between vehicle and barrier were categorised into two groups (Table I): the initial impact condition (i.e. impact velocity, impact angle, and overlap ratio) (Fig. 2); and the contact condition (i.e. the friction coefficient of tyre and road). Random uniform sampling was used to generate balanced large-scale ECP data. It has no strict limitation on the data size compared with grid sampling. Although, too much data is unnecessary because it would decrease the sample differences and increase the computational load.

TABLE I
CONTINUITY AND RANGE OF THE FIRST IMPACT FEATURES

Features	Continuity and range
Impact velocity (km/h)	Continuous: [25,65] [4]
Impact angle (deg)	Continuous: [-30,30] [5]
Overlap ratio (%)	Discrete: Seven types
Friction coefficient	Continuous: [0.2,0.8] [6]

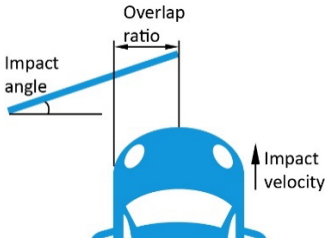

Fig. 2. Initial impact condition features explanation.

Second impact phase The longitudinal, lateral and yaw ECP of B-pillar measurement point were imported into the vehicle-occupant model. The airbag deployment time (t) was calculated according to longitudinal Δv (Eq. 1), and the exponential regression function was fitted with the EDR data of vehicle-to-vehicle frontal impact [7]. The seatbelt pretensioner trigger time had a 5 ms delay. The airbag would deploy only when the longitudinal Δv was greater than 19 km/h.

$$t = \mathrm{e}^{0.02327\Delta v + 3.760} \quad (1)$$

where Δv is the final velocity minus the initial velocity (km/h); t is the deployment time (ms).

Restraint system configurations and driver characteristics were used as the second impact features (Table II). Driver characteristics (Fig. 3) included body characteristics (i.e. height and BMI) and posture (i.e. recline angle and leaning angle). Twelve kinds of driver models were scaled from MADYMO Hybrid-III 50% male dummy model. Restraint system configurations included seating position (i.e. the distance from the front seat to the brake pedal), the use of knee airbag or airbag, and the seatbelt load limiter force level. Random uniform sampling was also used.

TABLE II
CONTINUITY AND RANGE OF THE SECOND IMPACT FEATURES

Features	Continuity and range
Driver height (m)	Discrete: [1.60 1.70 1.80]
Driver BMI	Discrete: [21 23.5 26 28.5]
Leaning angle (deg)	Continuous: [-8.6,8.6]
Recline angle (deg)	Continuous: [-20,20]
Seating position (m)	Continuous: [-0.142,0.142]
Knee airbag	Discrete: two types
Airbag	Discrete: two types
Load limiter force (kN)	Discrete: [0 3 4]

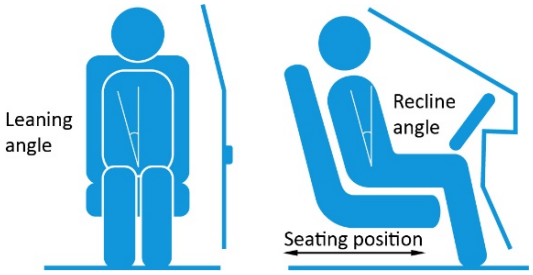

Fig. 3. Geometric parameters of the interior features.

Driver responses (outputs) Linear acceleration and angular velocity at head, force and moment at neck, acceleration and deflection at thorax were output. In particular, angular velocity was output to adopt BrIC to

assess injury risk of mTBI (mild Traumatic Brain Injury), although it has not yet been considered in many regulation tests.

Simulation validation cases National Automotive Sampling System/Crashworthiness Data System (NASS/CDS) provides a detailed record of nationwide crash samples throughout the United States. We filtered 23 eligible cases from NASS/CDS to verify the accuracy of the simulation model, namely, the accuracy of the numerical database. Fourteen male and nine female drivers were included. The driver age range was 39.08±13.7 years old, height range was 1.71±0.11 m, and BMI range was 24.46±4.48. The vehicle year ranged between 1986 and 2014. The impact velocity equalled to Barrier Equivalent Speed (BES), the seatbelt load limiter force was kept at 3 kN, and the recorded text information was transformed into discrete value for validation.

III. INITIAL FINDINGS

We built a frontal impact simulation model of TOYOTA Camry with VCS and MADYMO, and each full simulation case took 18 minutes on average (Intel i7-9700K 3.60GHz processor). The threshold for injury assessment was assumed to be 50% of probability, e.g. the final injury severity is AIS2, if AIS2 injury risk is higher than 50% while AIS3 injury risk is lower than 50%.

HIC, BrIC, N_{ij}, 3 ms clip thorax region peak acceleration, maximum chest compression and CTI were calculated as injury metrics at components and used to estimate AIS-level injury risk respectively, following [8]. No neck injury was observed in real-world accident cases or in simulation results. The head injury severity was decided by the most severe result between HIC and BrIC. The chest acceleration criterion tended to overestimate the chest injury severity, which is consistent with Maika *et al*. [9]. Conversely, the chest deflection criterion inclined to underestimate the chest injury severity. Therefore, the CTI was adopted as the chest injury predictor. Seventeen cases were correctly predicted, the simulation accuracy is 73.91% (91.30% if divided with AIS3+, e.g. the prediction is correct if the predicted and recorded injury severity are less than AIS3) (Table III).

For the two incorrectly predicted cases with serious injuries, the detailed accident information was investigated. The AIS3 chest injury in Case 179007091 was caused by hemo-/pneumothorax, beyond the prediction scope of CTI. Therefore, the prediction error was in fact an under estimation of AIS0 compared to the recorded rib fracture of AIS1. The underestimate of chest injury of Case 158010152 may stem from the aging effect as the driver's age was 59 years; the overestimate of head injury was generated by numerical penetration between the occupant head and the A-pillar, which is impossible in real-world scenarios.

TABLE III
VALIDATION RESULTS OF 23 REAL-WORLD ACCIDENT CASES (IV - IMPACT VELOCITY, IA - IMPACT ANGLE, SR - SLIGHTLY RECLINED (15 DEG), UR - UPRIGHT (0 DEG), AB - AIRBAG, KAB - KNEE AIRBAG, PT- PRETENSIONER)

Case ID	Initial condition		Restraint system configurations			Injury severity*	
	IV (km/h)	IA (deg)	Recline state	Airbag state	Seatbelt state	Head injury	Chest injury
178008782	51	10	SR	Off	On	AIS1 (AIS1)	AIS1 (AIS2)
179007091	32	20	SR	Off	On	AIS1 (AIS1)	AIS3 (AIS0)
151007963	34	-20	SR	AB	On	AIS0 (AIS1)	AIS1 (AIS0)
156008717	34	30	UR	Off	On	AIS0 (AIS0)	AIS1 (AIS0)
179007471	24	-30	SR	AB	Off	AIS0 (AIS0)	AIS0 (AIS0)
910004128	46	10	UR	AB	On+PT	AIS0 (AIS1)	AIS2 (AIS0)
774012054	41	0	SR	AB	Off	AIS0 (AIS0)	AIS0 (AIS0)
766013494	25	30	UR	AB	On+PT	AIS0 (AIS0)	AIS0 (AIS0)
748013751	31	0	SR	AB+KAB	On+PT	AIS0 (AIS1)	AIS0 (AIS0)
748014109	32	0	SR	AB+KAB	Off	AIS1 (AIS0)	AIS0 (AIS0)
773014835	33	-20	SR	AB+KAB	Off	AIS0 (AIS1)	AIS0 (AIS0)
208017576	25	-10	UR	AB+KAB	On+PT	AIS0 (AIS0)	AIS0 (AIS0)
159009744	46	10	UR	AB	Off	AIS1 (AIS0)	AIS0 (AIS2)
158010152	48	-30	SR	Off	Off	AIS2 (AIS5)	AIS5 (AIS2)

175014375	49	-10	UR	AB	Off	AIS1 (AIS2)	AIS1 (AIS2)
770016693	31	-25	SR	AB+KAB	Off	AIS0 (AIS0)	AIS0 (AIS0)
910002484	56	0	SR	AB	On+PT	AIS2 (AIS2)	AIS2 (AIS2)
765013235	39	-10	SR	AB+KAB	On+PT	AIS0 (AIS1)	AIS0 (AIS0)
774013754	25	30	SR	AB+KAB	On+PT	AIS1 (AIS1)	AIS0 (AIS0)
717016452	31	10	SR	AB	On+PT	AIS1 (AIS1)	AIS0 (AIS0)
771014519	39	10	SR	AB	On+PT	AIS0 (AIS1)	AIS1 (AIS0)
520016534	31	-30	SR	Off	On+PT	AIS0 (AIS1)	AIS0 (AIS0)
896018844	38	0	UR	AB+KAB	On+PT	AIS0 (AIS0)	AIS1 (AIS0)

* AIS0 and AIS1 were not distinguished; the predicted value is in parentheses.

IV. DISCUSSION

As the first step in training injury prediction models for occupant safety, the proposed simulation process allows us to readily generate a reliable large-scale driver injury severity database, which can go beyond the scope of FE modeling or the field accident data collection. It is to be further used to provide in-crash injury information that can be combined with near-crash data (e.g. NDD) for real-time injury severity prediction. The predictability of features and the diversity of crash pulses are considered in the present numerical database. In order to separate out the near-crash and in-crash phases, the considerations of features selection are twofold. First, it is practical to obtain the necessary input features in a real-time manner using prediction algorithms. For the first impact phase, the initial impact condition is vehicle kinematics-based and can be predicted with near-crash NDD. For the second impact phase, the features of driver characteristics and restraint system configurations are available via the sensors of the adaptive restraint system. Secondly, the information should be sufficient for accident reconstruction. The above satisfying injury validation results between simulation and real-accident prove that when the impacted object type is given (e.g. tree, sedan, or SUV), these features are adequate. Due to the lack of diversity, the crash pulse has been seldom used as a feature of driver injury severity prediction. The ECP, which is a simplification of the crash pulses of real-world accidents, can provide enough diversity. It is also a suitable intermediate variable for end-to-end prediction for the highly accurate injury outputs. Moreover, the relationship between driver injury severity and ECP, restraint system configurations and driver characteristics is valid, regardless of the credibility of the ECP. The knowledge gained from this numerical database can be easily adapted into real-world MVCs by the transfer learning method.

Several limitations must be noted. First, we have not yet considered the intrusion and low extremity postures, although the femur and tibia axial forces were validated. Secondly, the complex influence of population factors on injury tolerance (e.g. aging) has not yet been considered. Thirdly, for simplification purposes only rigid wall impact is used with the impact velocity equal to BES, rather than the more widely used Δv. Further research efforts are necessary to use other deformable barriers for vehicle-to-vehicle impact simulation so that the vehicle velocity can be used as impact velocity directly.

V. ACKNOWLEDGEMENTS

This work was supported in part by National Natural Science Foundation of China (51705276, 51675295), Tsinghua University Initiative Scientific Research Program (2019Z08QCX13), and National Key R&D Program of China (2017YFE0118400, 2018YFE0192900).

VI. REFERENCES

[1] Peter, T. S., *et al*., *Accid Anal Prev,* 2011.
[2] Bance, I., *et al.,* IRCOBI, 2019.
[3] Reichert, R., *et al.,* SAE, 2016.
[4] Hampton, C. E., *et al., AAAM,* 2009.
[5] Saeki, H., *et al., SAE*, 2004.
[6] Kordani, A. A., *et al., Civil Eng J,* 2018.
[7] German, A., *et al., AAAM,* 2007.
[8] Eppinger, R., *et al*., NHTSA, 2000.
[9] Maika, K., *et al*., ESV, 2013.